

**A PARAMETRIC EXAMINATION OF SOME PROPERTIES  
OF THE LOW-FREQUENCY AMBIENT-NOISE FIELD**

by

**I. A. Fraser**

**Defence Research Establishment Atlantic  
Canadian Department of National Defence  
Dartmouth, Nova Scotia, Canada**

**ABSTRACT**

Models for ship-generated ambient noise vary considerably in the detail required of their input data on sources and the environment. This paper describes a model that predicts ambient-noise levels and cumulative distribution functions for Poisson-distributed shipping. Representing statistically both the locations and source levels of the ships serves to minimize the input requirements. It then proves relatively easy to study parametrically the sensitivity of the predictions to propagation conditions, shipping densities, source-level distributions, and array directivity. The model is also well-matched to the limited environmental information often available for sea trials. Predictions will be compared with experimental data to illustrate the utility of the model.

**1 INTRODUCTION**

Many acoustic sea trials collect ambient-noise data in the frequency range of 10 to 250 Hz where ship-radiated noise is the dominant source mechanism. However, a very considerable effort is then required if enough information on the ship sources and on environmental effects is to be collected to permit the ambient-noise field to be modelled deterministically. Time and resources are very seldom available to do this. Then we must rely on statistical estimates of source levels and locations of ships, and upon transmission-loss model predictions, to provide the necessary input data for the ambient-noise model.

It is essential to have a thorough understanding of the limitations of the predictive capability of such models. How dependent is each aspect of the statistical prediction upon each of the input parameters? How much confidence can be placed in the model if environmental or shipping conditions change? Are all of the major influences on ambient-noise statistics accounted for correctly in the model? It is hoped that this paper and the ambient-noise model FLAN described herein will make significant progress towards answering these questions.

The model is similar to a few others<sup>1-3</sup> in that it divides the ocean into arbitrary areas within which transmission loss to a sensor is constant. The number of

ships in each of the areas is assumed to be a random variable (abbreviated rv) governed by Poisson statistics. Based on these assumptions and statistically distributed source levels (SL), we can estimate the zeroth and first order ambient noise statistics, i.e. mean, standard deviation (sd), and (cumulative) distribution function (cdf), where the cdf  $F(x)$  is related to the probability density function (pdf)  $f(y)$  by the following expression:

$$F(x) = \int_{-\infty}^x f(y) dy .$$

FLAN differs from the other models<sup>1-3</sup> to some extent in its ease of specifying input parameter values. It also uses a different procedure for specifying the areas governed by each independent Poisson distribution, and for convolving the contribution of each area to the total noise field.

A set of predictions is made in Section 3 to illustrate the influence of each adjustable parameter upon the noise statistics. To indicate that the model, using plausible input values, is able to reproduce experimental data, some of the examples are compared with data collected by DREA during sea trials. Section 4 briefly describes the the influence of horizontal directivity of an array of sensors upon the ambient-noise statistics. A summary of points covered and the main conclusions that stem from this study appear in Section 5.

## 2 THE MODEL

### 2.1 ASSUMPTIONS

In the FLAN model for ship-generated ambient noise, the emphasis is on making the input specification as simple as possible. In deference to this aim several assumptions are made. These assumptions are more easily visualized if reference is made to the map in Fig. 1, on which are defined some of the model parameters. The principal assumptions are as follows:

- (1) the ocean area of interest can be divided into a number of subareas, each with constant mean transmission loss to the receiving hydrophone;
- (2) transmission loss (TL), or more specifically, transmission efficiency (TE) defined by  $TE = 10^{-(TL/10)}$ , is independent of azimuth within a specified sector (in this paper  $360^\circ$  will be assumed for simplicity);
- (3) points (1) and (2) above suggest that the subareas should be annular in shape, as illustrated in Fig. 1, with the sensor or array located at their center;
- (4) the density of shipping (number per unit area  $Q$ ) is constant between arbitrary minimum and maximum range limits,  $R_{min}$  and  $R_{max}$ ,

- (5) the number of ships in a given annulus is an rv  $n_h$  drawn from a Poisson distribution, with a mean ship count of  $b_h$  in the  $h$ -th annulus;
- (6) each contributing class of ships is distributed uniformly throughout the area of interest so that the composite source-level distribution will prevail everywhere;
- (7) transmission loss will normally be assumed to increase as  $20 \log R$  up to transition range  $R_0$  and as  $10 \log R$  thereafter, with an additional attenuation proportional to range and specified by a coefficient  $\alpha$  (there is also provision for using TL calculated with a ray-trace model);
- (8) virtually any source-level distribution can be mocked up by combining  $m$  relatively narrow distributions of arbitrary mean source level and weighting factor;
- (9) the statistical predictions are representative of an ensemble average over a large number of statistically independent data samples.

## 2.2 MODEL DEVELOPMENT

The FLAN model is called upon principally to relate ship and environmental information to cumulative distribution functions of ambient-noise level. Therefore convolution of the density functions of input parameters will be expected to play an important role in the calculation. The USI model<sup>1</sup> uses ingenious techniques to avoid traditional convolution formulations. However, in the present case computational efficiency is not of primary concern. Rather, the emphasis is on minimizing the number of user-input parameters and easing the burden of specifying their values.

The discussion will first focus on the model development. Numerical procedures will be described in Section 2.3.

The method of dividing the ocean into annuli, each with constant transmission efficiency, was illustrated in Fig. 1. The model development proceeds from this point as shown schematically in Fig. 2. Four factors must be taken into account: the sources, the ocean medium for conducting the sound, the hydrophone sensor or array, and the data-analysis procedures.

The source power for each ship is an rv  $y$  drawn from the same density  $f(y)$ , as implied by Fig. 2. The selection of a form for the source-power pdf is governed by two requirements: (1) that its characteristic function be easily evaluated, and (2) that it be easily transformed into the log domain to facilitate comparison with published source-level distributions. Perhaps the simplest pdf to fulfill these conditions is the gamma density. In order to fit the great variety of possible SL density-function widths and shapes, it is necessary to provide for a weighted sum of gamma densities with different median values. The source-power pdf then has the following form:

$$f(y) = W_m \frac{c^{p+1}}{p!} y^p e^{-cy},$$

where in the present use  $p$  is arbitrarily chosen as 2,  $W_m$  is the weight for the  $m$ -th SL density, and

$$c = 3 \frac{\exp(-SL_{om}/g)}{TE_h} .$$

Here  $SL_{om}$  is the most probable value of the  $m$ -th source-level density and  $g = 10 \log e = 4.343$ .

As noted previously, the number of ships in each annulus,  $n_h$ , is also an rv (Poisson-distributed) with parameter  $b_h$ , the mean number of ships in the annulus. Since each annulus has the same width  $\Delta r$ ,  $b_h$  is proportional to the radius  $r_h$ . The medium modifies each noise source by the factor  $TE_h$ , so that the total noise power from annulus  $h$  becomes

$$x_h = \sum_{k=1}^{n_h} TE_h y_k .$$

The sensor provides to the processor an incoherent noise sum over all annuli:

$$z = \sum_{h=1}^H x_h .$$

Rather than convolving the pdfs of the rvs  $x_h$  to determine that of  $z$ , it is desirable to obtain and multiply together the characteristic functions (cf)s for the rvs in order to determine the ambient-noise power distribution. The process of summing the noise contributions from the various annuli is a "generalized Poisson process" as described by Papoulis (Ref. 4, page 575). The cf for  $x$  is then given by:

$$\Phi_{x_h}(\omega) = e^{b_h[\Phi_y(\omega TE_h) - 1]} ,$$

invoking the following property of cfs

$$\Phi_x = \Phi_y(\omega d) ,$$

where  $x = yd$ . The cf for  $z$  is

$$\Phi_z(\omega) = \prod_{h=1}^H \Phi_{x_h}(\omega) ,$$

and for  $y$  it is

$$\Phi_y(\omega TE_h) = \sum_{m=1}^M W_m \frac{(1 + j\omega TE_h/c)^3}{[1 + (\omega TE_h/c)^2]^3}.$$

### 2.3 NUMERICAL PROCEDURES

The inversion of  $\Phi_z(\omega)$  to form  $f(z)$  is accomplished by a discrete Fourier transform (DFT) using a procedure devised by Bird<sup>5</sup> and implemented at DREA by Walker<sup>6</sup>. Bird has shown that the DFT can be readily performed provided that the input densities are zero above an arbitrary limit  $Y$ . He then deduces appropriate values for  $Y$ , and for  $J$ , the number of terms in the finite approximation to the DFT for the general case.

Walker obtains<sup>6</sup>

$$F(z) = \frac{z}{Y} \sum_{l=-\infty}^{\infty} \Phi_z\left(\frac{2\pi l}{Y}\right) \text{sinc}\left(\frac{\pi lz}{Y}\right) e^{-j\pi lz/Y} \quad (1)$$

for  $z < Y$ , where  $\text{sinc}(z) = \sin(z)/z$ . (It is assumed that  $f(z) = 0$  if  $z > Y$ .) In Eqn. (1)

$$\Phi_z\left(\frac{2\pi l}{Y}\right) = \Phi_z(\omega).$$

In the case of a Poisson density it is necessary to truncate the probability density function (pdf) at a value  $Y$  to fulfill the above-mentioned condition. (In FLAN,  $Y$  was chosen to be equal to the mean noise level plus 15 dB.) Furthermore, the infinite sum over  $l$  in Eqn. (1) can not be accomplished in practice. Bird provides arguments suggesting that a practical rule for truncation is to determine  $J$ , the maximum value of  $l$ , from the following expression:

$$\frac{|\Phi_z(2\pi l/Y)|}{2\pi l} < 10^{-5}.$$

The expression used to evaluate  $F(z)$  in FLAN is Walker's Eqn. (A10):

$$F(z) = \frac{z}{Y} + 2 \sum_{l=1}^J \text{Re}\left[ \frac{\Phi_z(2\pi l/Y)}{j2\pi l} (1 - e^{-j2\pi lz/Y}) \right].$$

### 3 ANALYSIS PROCEDURES AND PREDICTIONS

#### 3.1 INPUT PARAMETERS

The program FLAN was run for a variety of plausible input-value combinations to test their influence upon the cdf, mean and standard deviation. The input variables are listed in Table 1.

TABLE 1. Input parameters for noise model FLAN

Q	Density of shipping (number/km <sup>2</sup> )
R <sub>min</sub>	Minimum analysis range (km)
R <sub>max</sub>	Maximum analysis range (km)
N	Mean total number of ships (if specified, governs maximum analysis range)
	Transmission-loss range dependence (generated externally by an acoustical model or defined by the following parameters:
R <sub>o</sub>	- crossover range (from spherical to cylindrical spreading loss)
α	- attenuation coefficient (dB/km)
Δr	Width of annulus (usually about 2 km)
	Source-level data:
M	- number of density functions
SL <sub>om</sub>	- most probable source level of each density function
W <sub>m</sub>	- weighting factor for each density function.

#### 3.2 PREDICTIONS--DEEP WATER

First we shall examine the dependence of the statistics upon shipping density, with other factors held constant at typical values, and transmission loss assumed to increase linearly with range. Four cdfs covering the range of light to heavy shipping densities are shown in Fig. 3. Several points can be made with respect to these cdfs:

- (1) the median noise level is approximately proportional to 10 log(shipping density): as the density of shipping rises, so does the mean ambient noise power;
- (2) the slopes of the cdfs (related to the sd) increase with decreasing shipping density Q: fewer ships provide less chance of averaging out the differences in source level, transmission loss and ship numbers;

- (3) the cdf is nearly log normal over 2 to 3 standard deviations, at least for the higher values of  $Q$ . In a small fraction of the samples and at short ranges a very few ships may be exposed to significantly different propagation conditions, such as the nearest convergence zone, or the direct-path region at a range less than  $R_o$ . This causes the curves to break near the 90th percentile. Since the source levels for all ships are drawn from the same pdf, all the cdfs of ambient noise will tend towards the same value at the high-noise limit.

Several examples showing this break in the cdf are provided in Fig. 4 for two types of propagation: on the left for convergence zones, and on the right for a smoothly increasing dependence of TL upon range. The variation of cdf shape with changing  $R_{min}$  points to nearby ships as the source of the curvature.

In deep water the mean and standard deviation of the noise field appear to depend most strongly upon the mean number of ships  $N$ . This dependence is examined with the aid of FLAN predictions in Fig. 5. The mean ship population contributing to the noise field is governed principally by  $Q$ , the shipping density, and by the upper range limit  $R_{max}$ . All other model parameters are held constant at representative values. It is clear that the major influence on sd is the value of  $N$ . For example, a change in ship density  $Q$  from 1.0 to 0.2 ships/ $10^4$  km<sup>2</sup> is seen to change sd by only 0.25 dB, provided that a corresponding change is made in  $R_{max}$  to hold  $N$  constant. It is interesting to note that the ambient-noise sd curves in Fig. 5 follow a trend similar to the sd of total ship count, where the latter is assumed to obey Poisson statistics.

A major concern in ambient-noise studies is the difficulty of specifying source-level distributions with any degree of confidence. The influence of several plausible source-level pdfs upon the sd of ambient-noise level is displayed in Fig. 6. The curves relating ambient noise sd to source-level sd were calculated for a single source-level pdf shape, namely that of Case 2 in the upper left corner of the diagram. Larger standard deviations are obtained by stretching the pdf to cover a larger range of source levels. The three source-level pdfs illustrated (Cases 1 to 3) were chosen to assess the effect of extreme changes in the density function shape upon the sd of ambient noise. The results for a  $Q$  of 1 ship/ $10^4$  km<sup>2</sup> and a source-level sd of 9 dB are indicated by crosses. In all cases tested, quite drastic changes in shape or in sd of the source-level pdfs were necessary in order to produce even modest changes in the ambient-noise sd.

Next we present a cursory examination of the effect of transmission-loss trends upon the statistics of interest. Several plausible deep-water range dependencies of TL are illustrated in Fig. 7. Two curves, labeled Labrador Sea and Mid-Atlantic were generated by a ray-trace program for specific ocean areas. The other three curves reflect various combinations of  $R_o$  and  $\alpha$ . Predictions of cdf shape have been derived for the four lowest curves in Fig. 7 and are displayed in Fig. 8. (The Labrador Sea case will be deferred to Fig. 9.) The variations in shape and slope of the cdfs are seen to be quite weak, considering the large variations in  $R_o$  and in  $\alpha$ . When  $\alpha$  is greatest, the influence of the many distant ships is diminished relative to those nearby. This increases the ambient-noise variability, i.e. steepens the cdf

slope. The effect is evident in Fig. 8. Little dependence of the cdf on  $R_0$  is observed, however, except above the 90th percentile. For the convergence-zone propagation (mid-Atlantic TL profile), both the slope of TL and of the cdf are most closely aligned with the geometric cases for which  $\alpha = 0.01$  dB/km.

Referring again to Fig. 7, we observe a large offset between TL in the Labrador Sea and that typical of the mid-Atlantic. If all other factors are assumed equal, then we would expect the mean ambient-noise level to be many decibels higher in the Labrador Sea environment. The cdf predictions for the two locations are represented by the top and bottom curves for equal densities of  $1 \text{ ship}/10^4 \text{ km}^2$  in Fig. 9. The sd of 1.55 dB for the lowest curve is quite typical of measurements near Bermuda<sup>7</sup>. However, DREA data (represented by dots in Fig. 9) collected in the Labrador Sea imply a much lower ambient-noise level and steeper cdf slope than that represented by the top curve. The good fit provided by the middle curve was obtained simply by reducing the shipping density by a factor of 5, and the ocean-basin size by 30%. Both changes are quite plausible. How much the source-level densities differ in practice, and how significant are different shipping and fishing patterns is, of course, much more difficult to assess.

### 3.3 PREDICTIONS--SHALLOW WATER

The shallow-water acoustical environment requires some changes in scale to be made to input parameters of the FLAN model. Transmission loss at short ranges tends to be less than in deep water, but often is subject to a relatively large attenuation as range increases. These differences in TL can be accommodated by reducing  $R_0$  and increasing  $\alpha$ , relative to their deep-water values. (DREA has been cataloging much of Canada's eastern shallow-water area in terms of these parameters.)

It is also anticipated that  $R_{\text{max}}$  should be much smaller in the confined continental shelf areas than in the deep ocean basins. A value of  $R_{\text{max}} = 200$  km was chosen for this study.

Source levels of fishing vessels generally are somewhat smaller than those for merchant ships. However, during fishing operations their radiated noise levels can be extremely high and quite variable.

The preceding factors all tend to increase the slope of cdfs relative to their typical deep-water values. A comparison of two cases for which data are available is made in Fig. 10. The shallow-water data were obtained by DREA in an area characterized by heavy shipping; the deep water data were obtained off Canada's east coast. Historical shipping densities were used in the model predictions, together with the source level density function illustrated as Case 2 in Fig. 6.  $R_{\text{max}}$  took on values of 750 km and 200 km for, respectively, the deep and shallow-water cases. The only parameter adjusted to provide the model fits shown in Fig. 10 were the mean values of the two source-level pdfs. The main factor contributing to the steepness of the shallow-water cdf is the elimination of contributions normally made by the many ships beyond 200 km range in deep-water areas.



The effect of variations in attenuation coefficient,  $\alpha$ , upon the cdf is displayed in Fig. 11. Since  $\alpha$  at low frequencies can be an order of magnitude greater in shallow water than in deep, its effect upon the cdf can be significant. As in the deep-water case (Fig. 8), the cdf becomes steeper as  $\alpha$  increases. A low-noise limit must be reached, however, as the shipping noise drops to zero, leaving only wind-generated noise in its stead.

#### 4 ARRAY DIRECTIVITY

The directional sensitivity (directivity) of an array of sensors can significantly influence the low-frequency ambient-noise statistics. For example, a narrow horizontal beam will reduce the number of contributing ships from an isotropic shipping distribution by the ratio of beamwidth to  $360^\circ$  (or  $180^\circ$  in the case of a line array). Not only is the mean noise power reduced by this factor, but the cdf slope, and consequently the sd, are increased by an amount that can be assessed by reference to Figs. 3 and 5, which show the influence of mean ship count upon cdf shape and upon sd, respectively. The effect of sidelobe structure requires special attention, and will not be addressed in this paper.

#### 5 SUMMARY AND CONCLUSIONS

A parametric ambient-noise model FLAN has been developed to assess the impact of variations in ship source levels and numbers, of transmission loss, and of sensor directivity upon the first-order statistics of ambient noise at low frequencies. A special effort has been made to minimize the number of input parameters and the effort required to specify their values, possibly at the expense of generality. This was done (1) to match the model's input requirements to the many experimental situations where little is known about the ships contributing to the noise field and the prevailing sound-transmission conditions, and (2) to make it easy to vary each parameter in a systematic manner to assess its impact upon the statistics of ambient noise.

The principal conclusions reached in the study are:

- (1) a wide variety of experimental data can be fit by such a model,
- (2) good model fits to experimental cdfs do not imply an unambiguous set of input-parameter values,
- (3) under many conditions the cdf of ambient noise is predicted to be log normal over two to four standard deviations,
- (4) the sd of ambient noise is principally dependent upon the number of ships contributing to the noise field,
- (5) in the case of directional arrays the number of ships contributing strongly to the noise field is diminished, so that the sd tends to become larger,

- (6) the sd of ambient noise is weakly dependent upon the source-level pdf of contributing ships, upon  $R_{\min}$ , and upon  $R_0$ ,
- (7) the shape of the cdf (as opposed to its slope) draws away from log-normal behavior as  $R_{\min}$  and  $Q$  decrease, and as  $\alpha$  increases,
- (8) shallow-water cdfs tend to be much steeper in slope than those for deep water, primarily because of the smaller region over which ships can contribute to ambient noise.

Extensions of the model to include explicitly the effect of shipping lanes, convoys, azimuthal dependence of transmission loss, and TL fluctuations can be envisaged, in order to increase its ability to cope with realistic environments. The cost of such improvements will be additional complexity in the input specification.

## 6 REFERENCES

1. R.L. Jeanette, E.L. Sander, L.E. Pitts, "The USI noise model, Version 1", Underwater Systems Inc. Report Nos. USI-APL-R-8 and 9 (April 1977); as described in "Review of models of beam-noise statistics", Science Applications Inc. Report No. SAI-78-696-W/A (Nov. 1977).
2. B.J. McCabe, "Ambient noise effects in the modeling of detection by a field of sensors", Daniel H. Wagner, Assoc. Report, Paoli, Pa. (5 Nov. 1976).
3. M. Moll, R.M. Zeskind, F.J.M. Sullivan, "Statistical measures of ambient noise: algorithms, program, and predictions", Bolt Beranek and Newman Report No. 3390, Arlington, Va. (11 June 1977).
4. A. Papoulis, Probability, Random Variables, and Stochastic Processes (McGraw-Hill, New York, 1965).
5. J.S. Bird, "Calculating detection probabilities for radar and sonar systems that employ non-coherent integration", IEEE Trans. Aerosp. Electron. Syst., accepted for publication.
6. R.S. Walker, "The detection performance of FFT processors for narrowband signals", DREA Technical Memorandum 82/A, Dartmouth (Feb, 1982).
7. A.J. Perrone, "Deep-ocean ambient-noise spectra in the northwest Atlantic", J. Acoust. Soc. Amer. 46, 762 (1969).

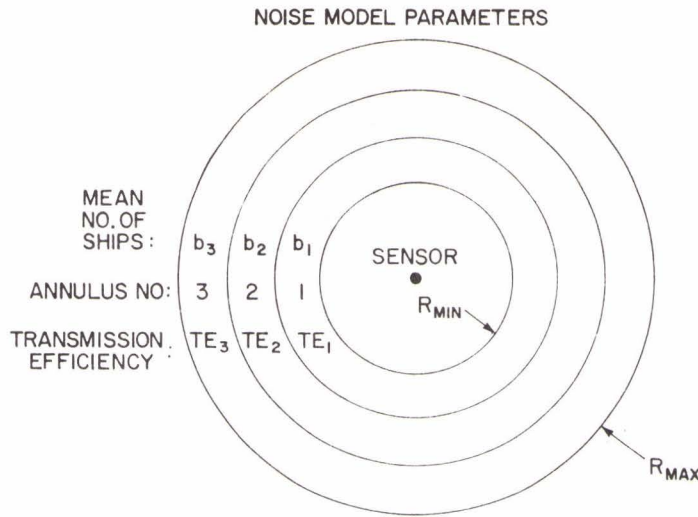


FIG. 1  
MAP OF OCEAN AREA DEFINING NOISE-MODEL PARAMETERS

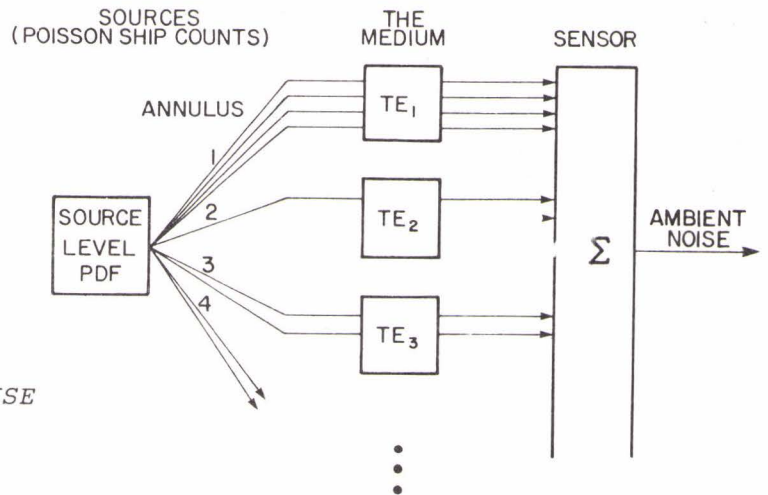


FIG. 2  
SCHEMATIC DIAGRAM OF FLAN NOISE MODEL

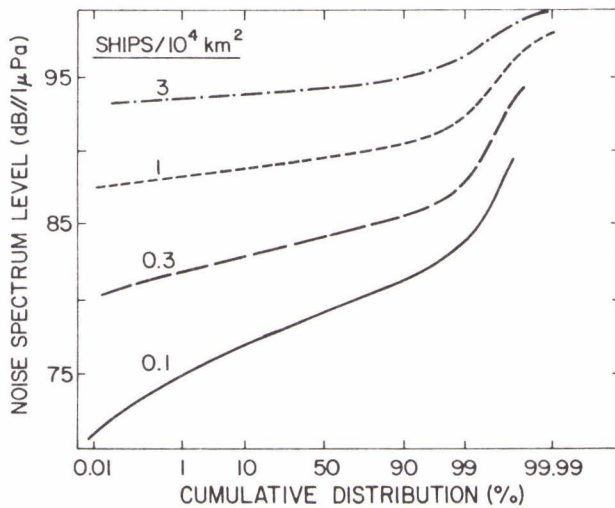


FIG. 3  
EFFECT OF SHIPPING DENSITY UPON THE CUMULATIVE DISTRIBUTION FUNCTION OF AMBIENT NOISE

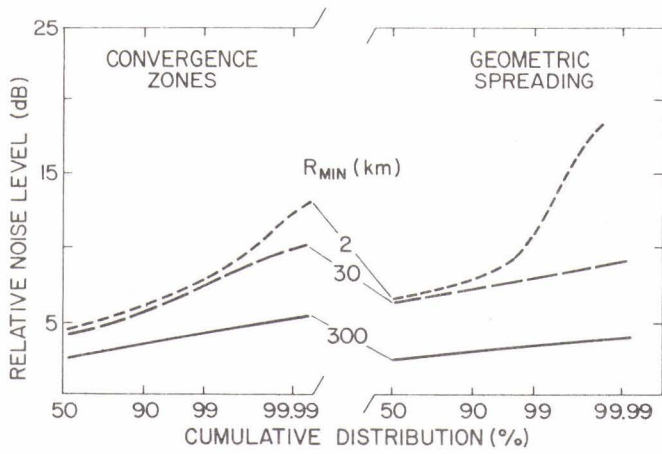


FIG. 4  
EFFECT OF MINIMUM CUTOFF RANGE  
UPON CUMULATIVE DISTRIBUTIONS  
IN TWO OCEAN ENVIRONMENTS

FIG. 5  
EFFECT OF MEAN SHIP POPULATIONS  
UPON THE AMBIENT-NOISE STANDARD  
DEVIATION

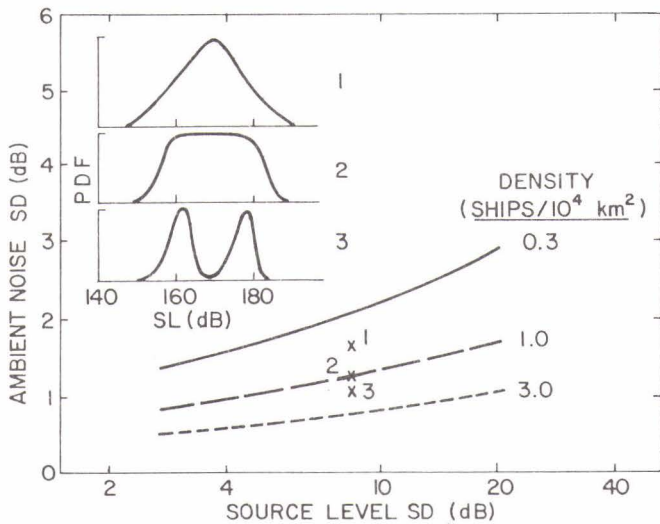
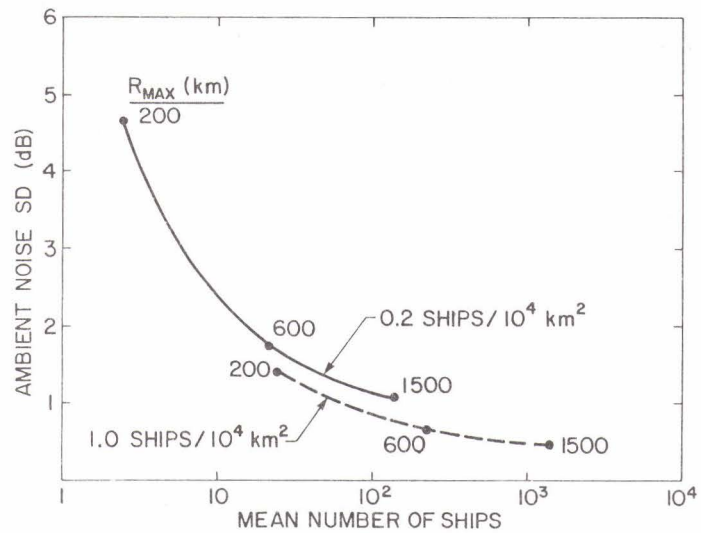


FIG. 6  
EFFECT OF SOURCE-LEVEL PROBABILITY  
DENSITY FUNCTION UPON THE AMBIENT-  
NOISE STANDARD DEVIATION

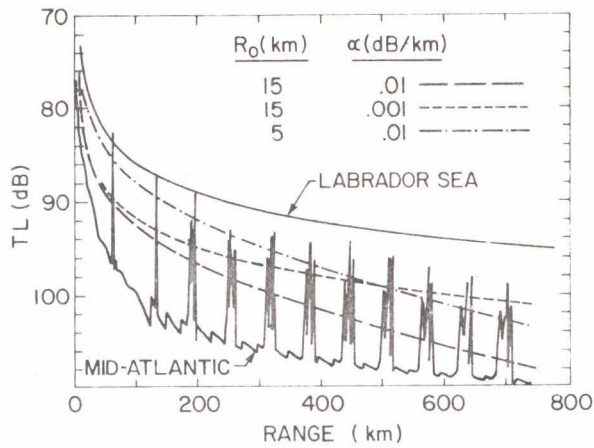


FIG. 7  
SOME TYPICAL TRANSMISSION-LOSS  
RANGE DEPENDENCES

FIG. 8  
CUMULATIVE DISTRIBUTION FUNCTIONS  
ASSOCIATED WITH THE TRANSMISSION-  
LOSS CURVES OF FIG. 7

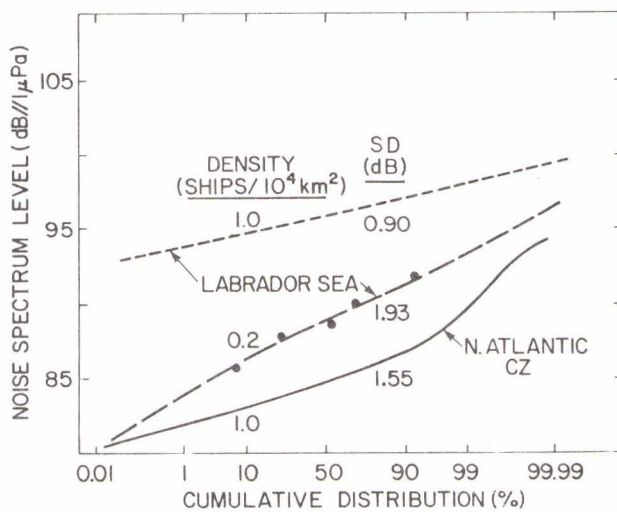
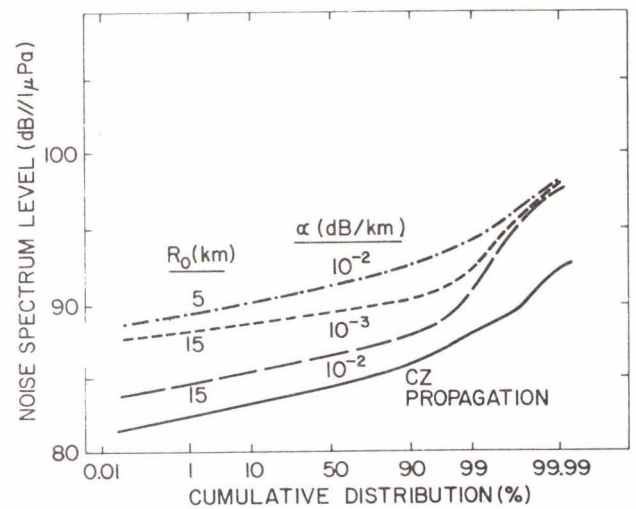


FIG. 9  
COMPARISON OF CUMULATIVE DISTRI-  
BUTION FUNCTIONS FOR THE LABRADOR  
SEA AND AN OCEAN AREA FURTHER  
SOUTH

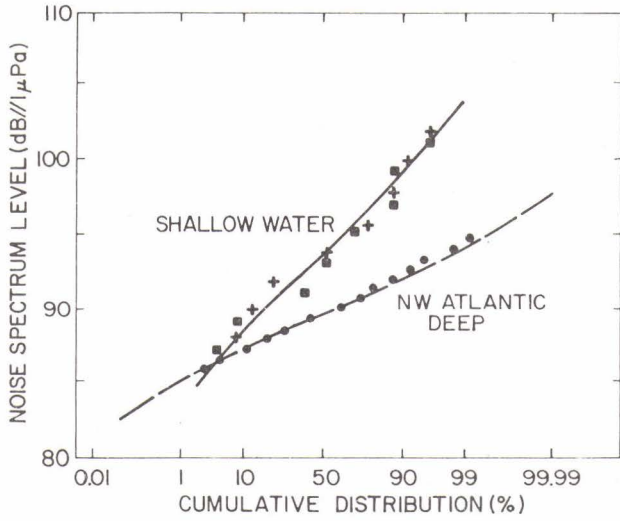


FIG. 10  
COMPARISON OF SHALLOW WATER AND DEEP WATER CUMULATIVE DISTRIBUTION FUNCTIONS, WITH SYMBOLS REFERRING TO DREA EXPERIMENTAL DATA

FIG. 11  
EFFECT OF ATTENUATION COEFFICIENT UPON THE CUMULATIVE DISTRIBUTION FUNCTION IN A SHALLOW WATER AREA

